crystals

MDPI

Article

Identification, Characterization, and Preliminary X-ray Diffraction Analysis of a Novel Esterase (*Sc*Est) from *Staphylococcus chromogenes*

Jisub Hwang [1,2,†], Sangeun Jeon [3,†], Min Ju Lee [1], Wanki Yoo [4], Juwon Chang [3], Kyeong Kyu Kim [4], Jun Hyuck Lee [1,2], Hackwon Do [1,2,*] and T. Doohun Kim [3,*]

1 Research Unit of Cryogenic Novel Material, Korea Polar Research Institute, Incheon 21990, Korea; hjsub9696@kopri.re.kr (J.H.); minju0949@kopri.re.kr (M.J.L.); junhyucklee@kopri.re.kr (J.H.L.)
2 Department of Polar Sciences, University of Science and Technology, Incheon 21990, Korea
3 Department of Chemistry, Graduate School of General Studies, Sookmyung Women's University, Seoul 04310, Korea; sangeun94@sookmyung.ac.kr (S.J.); cjw1423@naver.com (J.C.)
4 Department of Molecular Cell Biology, Samsung Biomedical Research Institute, Sungkyunkwan University School of Medicine, Suwon 440746, Korea; vlqkshqk61@skku.edu (W.Y.); kyeongkyu@skku.edu (K.K.K.)
* Correspondence: authors: hackwondo@kopri.re.kr (H.D.); doohunkim@sookmyung.ac.kr (T.D.K.)
† These authors contributed equally to this work.

Abstract: Ester prodrugs can develop novel antibiotics and have potential therapeutic applications against multiple drug-resistant bacteria. The antimicrobial activity of these prodrugs is activated after being cleaved by the esterases produced by the pathogen. Here, novel esterase *Sc*Est originating from *Staphylococcus chromogenes* NCTC10530, which causes dairy cow mastitis, was identified, characterized, and analyzed using X-ray crystallography. The gene encoding *Sc*Est was cloned into the *p*VFT1S vector and overexpressed in *E. coli*. The recombinant *Sc*Est protein was obtained by affinity and size-exclusion purification. *Sc*Est showed substrate preference for the short chain length of acyl derivatives. It was crystallized in an optimized solution composed of 0.25 M ammonium citrate tribasic (pH 7.0) and 20% PEG 3350 at 296 K. A total of 360 X-ray diffraction images were collected at a 1.66 Å resolution. *Sc*Est crystal belongs to the space group of $P2_12_12_1$ with the unit cell parameters of a = 50.23 Å, b = 68.69 Å, c = 71.15 Å, and $\alpha = \beta = \gamma = 90^\circ$. Structure refinement after molecular replacement is under progress. Further biochemical studies will elucidate the hydrolysis mechanism of *Sc*Est. Overall, this study is the first to report the functional characterization of an esterase from *Staphylococcus chromogenes*, which is potentially useful in elaborating its hydrolysis mechanism.

Keywords: carboxylesterase; *Staphylococcus chromogenes*; X-ray crystallography

check for updates

Citation: Hwang, J.; Jeon, S.; Lee, M.J.; Yoo, W.; Chang, J.; Kim, K.K.; Lee, J.H.; Do, H.; Kim, T.D. Identification, Characterization, and Preliminary X-ray Diffraction Analysis of a Novel Esterase (*Sc*Est) from *Staphylococcus chromogenes*. *Crystals* **2022**, *12*, 546. https://doi.org/10.3390/cryst12040546

Academic Editor: Waldemar Maniukiewicz

Received: 27 February 2022
Accepted: 2 April 2022
Published: 13 April 2022

Publisher's Note: MDPI stays neutral with regard to jurisdictional claims in published maps and institutional affiliations.

Copyright: © 2022 by the authors. Licensee MDPI, Basel, Switzerland. This article is an open access article distributed under the terms and conditions of the Creative Commons Attribution (CC BY) license (https://creativecommons.org/licenses/by/4.0/).

1. Introduction

Multiple drug resistance (MDR) bacteria are an emerging global threat that potentially imposes healthcare and economic issues [1,2]. The production of drug-inactivating enzymes, such as β-lactamase and aminoglycoside modifying enzymes [3], drug elimination from the cell, mutation of an existing target, and acquisition of a target by-pass system have been proposed as major MDR resistance mechanisms. Therefore, the necessity for discovering and developing novel antibiotics with unconventional modes of action has increased in order to overcome these resistance mechanisms [4].

One of the strategies to avoid MDR is antibacterial prodrugs that are pharmacologically inactive and are cleaved by bacterial enzymes to become active antibiotics [5]. Antibacterial prodrugs are synthesized by adding functional groups to the antibiotic skeleton and may have multiple advantages [5]. For example, adding a lipophilic pivaloyloxymethyl to cephalosporin cefditoren increases its absorption in the small intestine [6]. Ester is also a functional group that is added to antibiotics to increase the delivery efficiency, cell permeability, and oral bioavailability of the prodrug [7,8]. Carbenicillin, carfecillin (phenyl

ester), and carindacillin (indanyl ester) are some ester-containing antimicrobial prodrugs [9]. Pathogen specificity is another advantage of ester prodrugs. Since such antibacterial prodrugs are transformed by the cytosolic esterase specifically produced by the pathogen, the pathogen is selectively executed [10].

Previously, human esterases were studied for their function in prodrug activation [11]. However, the application of human esterase for antibiotic prodrug activation is limited due to its esterase-dependent localization and expression. Alternatively, analyzing the substrate selectivity and activity of bacterial esterases has provided crucial details for targeting potential antibiotic prodrugs to develop novel antibiotics for the treatment of MDR [5,7,10,12]. Bacterial esterases have a canonical α/β-hydrolase fold that consists of a core β-sheet surrounded by α-helices to catalyze the hydrolysis (EC 3.1.1.X) of a variety of substrates containing ester groups. The esterases use a catalytic triad comprising a nucleophilic serine, a base histidine, and an activating acidic residue (Asp/Glu) to catalyze the hydrolysis of the ester to a carboxylic acid and alcohol. Despite having the same configuration as the enzyme hydrolase and a high degree of sequence homology, esterases have distinct substrate specificities [13–15]. Therefore, pathogenic esterases need to be functionally investigated, whereas the biochemical and structural studies may provide valuable information for designing species-specific antimicrobial ester prodrugs. This preliminary study focuses on the substrate specificity and function of esterases derived from pathogens. Herein, we have analyzed the distribution of esterases and lipases across the genome of *Staphylococcus chromogenes* NCTC10530, the prevalent bacterial pathogen causing dairy cow mastitis. Furthermore, the carboxylesterase annotated as *Sc*Est has been purified, its biochemical properties have been investigated, and preliminary X-ray studies have been conducted.

2. Materials and Methods

2.1. Phylogenetic Analysis

The subfamily of *Sc*Est was analyzed using a phylogenetic tree based on full-length protein sequences of several lipolytic enzymes that are already classified into specific subfamilies [16–18]. A total of 69 protein sequences, including *Sc*Est and other proteins from the *S. chromogenes strain* NCTC10530 were used for multiple sequence alignment using ClustalX [19]. The neighbor-joining method was used to generate a phylogenetic tree using the MEGA-X [20].

2.2. Gene Cloning, Expression, and Purification of Recombinant ScEst Protein

The gene encoding *Sc*Est (GenBank ID: SUM13810) was amplified by PCR and cloned into the *p*VFT1S plasmid between the *BamH*I and *Xho*I restriction sites. The cloned sequence was verified using Sanger sequencing using T7 promoter and terminator primers. *E. coli* BL21 (λDE3) was transformed with the recombinant plasmid harboring N-terminal 6xHis-tagged *Sc*Est for protein overexpression (Table 1). A single colony from the Luria Bertani (LB) agar plate containing kanamycin was inoculated as a seed culture and grown overnight. The seed culture (20 mL) was inoculated into 1 L of culture medium and kanamycin (50 μg mL^{-1}) and incubated at 37 °C at 150 rpm. When the OD_{600} of the culture reached 0.4, protein overexpression was induced by adding 1.0 mM isopropyl β-D-1-thiogalactopyranoside (IPTG). The cells were further incubated at 37 °C for 4 h, and harvested by centrifugation at 6000× *g*. The cell pellets were resuspended in a lysis buffer (20 mM Tris-HCl [pH 8.0], 500 mM NaCl, and 20 mM imidazole) and disrupted by sonication (Vibra-Cell™, Sonics & Materials, Inc., Danbury, CT, USA) for 30 min at 35% amplitude (on for 2 s and off for 4 s). The soluble fraction of protein was separated by centrifugation at 20,000× *g* for 40 min.

Recombinant *Sc*Est was purified via a two-step purification process. First, the His-tag-based purification was performed using a His-trap™ FF column (GE Healthcare, Chicago, IL, USA). The supernatant containing the recombinant *Sc*Est was loaded onto the column, and the resin was washed with 10 column volumes of washing buffer. The remaining recombinant *Sc*Est was eluted with two column volume elution buffer (20 mM Tris-HCl

[pH 8.0], 500 mM NaCl, 300 mM imidazole). The elute was then concentrated to 5 mL and treated with thrombin for three days at 4 °C in a rotating incubator to cleave the His-tag. For the second purification, HiPrep™ Sephacryl® S-200 HR (Cytiva, Marlborough, MA, USA) connected to an ÄKTA™ Start chromatography system (GE Life Sciences, Piscataway, NJ, USA) was equilibrated with a buffer composed of 20 mM Tris-HCl (pH 8.0), 200 mM NaCl, and 1 mM EDTA, and the protein sample was loaded onto the column. The column was calibrated using cytochrome C (12.4 kDa), carbonic anhydrase (29 kDa), alcohol dehydrogenase (150 kDa), and β-amylase (200 kDa). K_{av} was calculated by $(V_s - V_o)/(V_t - V_o)$, where vs. = elution volume, V_o = column void volume, V_t = column volume. The purity and concentration of the recombinant *Sc*Est were validated using SDS-PAGE and the Bradford protein assay, respectively.

Table 1. Recombinant *Sc*Est protein attributes.

***Sc*Est**	
Source organism	*Staphylococcus chromogenes* strain NCTC10530
DNA source	Genomic DNA
Cloning vector	pVFT1S
Expression host	*Escherichia coli* BL21(DE3)
Amino acid sequence	MKIQLPKPFLFEEGKRAVLLLHGFTGNSSDVRQLG RFLQKKGYTSYAPHYEGHAAPPEEILKSSPHVWY KDALDGYDYLVDKGYDEIAVAGLSLGGVFALKLS LNRDVKGIVTMCSPMYIKTEGSMYEGVLEYARNF KKYEGKDETTIEREMQAFHPTSTLRELQETIQSV RDHVEDVIEPLLVIQAEQDEMINPDSANVIYNEA ASDEKHLSWYKNSGHVITIDKEKEDVFEEVYQFLESLDWSE

2.3. Enzymatic Analysis

The substrate specificities of *Sc*Est were measured using various *p*-nitrophenyl esters, including *p*-nitrophenyl acetate (*p*NP-C_2), *p*-nitrophenyl butyrate (*p*NP-C_4), *p*-nitrophenyl hexanoate (*p*NP-C_6), *p*-nitrophenyl octanoate (*p*NP-C_8), and *p*-nitrophenyl decanoate (*p*NP-C_4), obtained from Sigma-Aldrich (St. Louis, MO, USA). The esterase activity with acyl carbon chains of various lengths was evaluated by monitoring the *p*-nitrophenol (*p*NP) in the solution spectrophotometrically [21]. Storage buffer (1 mL) containing 20 mM Tris-HCl (pH 8.0), 200 mM NaCl, and 1 µg *Sc*Est was prepared, and the reaction was initiated by mixing an equal volume of the substrate (final 0.12 µM). The final concentration of acetonitrile in the reaction mixture kept to 5% to avoid micelle formation of substrates with longer acyl chains. The enzyme reactions were analyzed at 405 nm using an Epoch™ 2 microplate spectrophotometer (BioTek Instruments, Winooski, VT, USA), using the storage buffer as control. Three independent measurements were used to represent the activity data.

2.4. Crystallization, Data Collection, and Structural Analysis

Commercially available crystallization solutions, MCSG I-IV (Anatrace Inc., Maumee, OH, USA), and JCSG™ and PGA Screen™ (Molecular Dimensions Inc., Altamonte Springs, FL, USA) were used to screen the crystallization conditions of *Sc*Est. The sitting-drop vapor diffusion method was set up by mixing 300 nL of solution and an equal volume of protein (25 mg mL^{-1}) against 80 µL of solution in the reservoir using a mosquito® liquid-handling robot (TTP Labtech Ltd., Hertfordshire, UK). Subsequently, multiple optimizations using 24-well plates were further carried out to obtain a decent size and quality of crystals. The crystallization data are presented in Table 2.

The single crystal of *Sc*Est was cryoprotected using a mixture of crystallization solution where the crystal of ScEst grew and glycerol (25% *w*/*v*) to prevent the crystal from being frozen under a liquid nitrogen stream. The crystal was then mounted on a sample holder. A total of 360 diffraction images were collected at the synchrotron Beamline 7A of the

Pohang Accelerator Laboratory (PAL, Pohang-si, Korea) by rotating at 1° oscillation per frame. The dataset was indexed, integrated, and scaled using the HKL-2000 software package (HKL Research Inc., Charlottesville, VA, USA). The phase of the *Sc*Est structure was successfully determined using the carboxylesterase Est30 (PDB code: 1TQH) with the molecular replacement method. The X-ray diffraction results are listed in Table 3.

Table 2. Initial crystallization conditions and optimization method.

Method	Vapor Diffusion
Plate type for screening	96-well sitting drop MRC plate (Molecular dimension, UK)
Composition of reservoir solution	0.2 M Ammonium citrate tribasic (pH 7.0), 20% PEG 3350
Plate type for optimization	24-well hanging drop plate, (Molecular dimension, UK)
Composition of optimal solution	0.25 M Ammonium citrate tribasic (pH 7.0), 20% PEG 3350
Temperature (K)	296
Protein concentration (mg/mL)	4.3
Composition of protein solution	20 mM Tris-HCl (pH 8.0), 200 mM NaCl
Volume and ratio of drop (protein: solution)	2.0 µL, 1:1
Volume of reservoir (µL)	500

Table 3. X-ray diffraction data.

Data Collection	
Wavelength (Å)	0.9793
X-ray source	PAL 7A
Rotation range per image (°)	1
Exposure Time (s)	1
Space group	$P2_12_12_1$
Unit-cell parameters (Å, °)	a = 50.23, b = 68.69, c = 71.15 α = 90, β = 90, γ = 90
Resolution range (Å) [a]	50–1.66 (1.69–1.66)
No. of observed reflections [a]	402,244 (19,564)
No. of unique reflections [a]	29,406 (1471)
Completeness (%) [a]	99.3 (100)
Redundancy [a]	13.7 (13.3)
R_{sym} [a,b]	0.112 (1.202)
R_{meas} [c]	0.117 (1.250)
I/σ [a]	62.3 (4.0)
CC(1/2) (%)	99.6 (82.8)
Wilson B factor (Å^2)	24.66
Matthews coefficient	2.18

[a] Values in parentheses correspond to the highest-resolution shells. [b,c] $R_{sym} = {}_{hi} | I(h)_i - <I(h)> | / {}_{hi} I(h)_i$, $R_{meas} = \Sigma hkl \{N(hkl)/[N(hkl) - 1]\} 1/2 {}_i | Ii(hkl) - | / hkl_i I(hkl)$, where I is the intensity of reflection h, $_h$ is the sum over all reflections, and $_i$ is the sum over i measurements of reflection h.

3. Results and Discussion

3.1. Lipolytic Enzymes of S. chromogenes NCTC10530 and Classification of ScEst

Initially, the bacterial esterases and lipases were classified into eight families (I–VIII) and six subfamilies, all of which belong to Family I, based on the biochemical properties and sequence similarity known as the gold standard classification [17]. Recently, several newly identified lipolytic enzymes have been incorporated into the classification system, resulting in its expansion to 35 families and 11 lipase subfamilies [18].

In this study, a total of 27 putative lipolytic enzymes were identified from the in silico analysis of the genome sequence of *S. chromogenes* strain NCTC10530. These enzyme sequences were aligned with the categorized enzymes (Figure 1). Among the putative lipolytic enzymes, *Sc*Est was found to be homologous to Family XIII, specifically with thermostable carboxylesterase Est30 from *Geobacillus stearothermophilus* (AAN81911, 62.30% identity), EstOF4 from *Bacillus* sp. (AGK06467, 56.50% identity), and EstB2 from *Bacillus* sp. (AAT65181, 58.54% identity).

Multiple sequence alignment revealed that the active site of *Sc*Est shares a consensus sequence G-X-S-X-G, characteristic of the esterase/lipase family (Figure 2). *Sc*Est displayed high sequence similarity with the Family XIII proteins. However, a unique region was also identified in *Sc*Est. The amino acid sequence 103–SLNRD–107 follows the active loop in *Sc*Est in contrast to its orthologs, which have GYTVLP in the corresponding region (Figure 2). Since this site is in the vicinity of the active site, *Sc*Est may have different specificities for substrate recognition or activity. Overall, the phylogenetic and sequence analyses confirmed that *Sc*Est belongs to the XIII family but harbors a unique sequence, which may lead to a distinctive function.

3.2. Biochemical Characterization of ScEst

To confirm the esterase activity, *Sc*Est was expressed and purified using a two-step purification process. His-Tag-affinity purification followed by size-exclusion chromatography yielded the recombinant *Sc*Est protein with high purity (>95%), and a molecular weight similar to the calculated molecular weight of 29.2 kDa (Figure 3A). The molecular weight of *Sc*Est estimated by size-exclusion chromatography on FPLC was consistent with the anticipated size of the dimer (Figure 3B). The esterase activity of *Sc*Est assessed using *p*-nitrophenyl esters (*p*-NP) indicated that *Sc*Est has a substrate preference for acyl derivatives with a short chain length, and the activity declined as the size of the acyl hydrocarbon chain of the substrates increased. When the activity of *Sc*Est against *p*-nitrophenyl acetate (C2) was considered 100%, the relative activity was approximately 50% and 20% against *p*-nitrophenyl butyrate (C4) and *p*-nitrophenyl hexanoate (C6), respectively. Substrates longer than hexanoate did not show any measurable activity.

3.3. X-ray Crystallographic Study of ScEst

To determine the three-dimensional structure of *Sc*Est, crystallization screening using more than 1600 conditions, X-ray diffraction experiments, and initial model building were performed. After multiple crystallization refinements, the best single crystal was obtained with 0.25 M ammonium citrate (pH 7.0) and 20% (*w*/*v*) PEG 3350 (Figure 4A). The single crystal was cryoprotected by a brief soaking in 25% glycerol-based cryoprotectant solution and mounted under a liquid nitrogen stream at 100 K. The full coverage of 360 diffraction images was obtained at the highest resolution of 1.66 Å (Figure 4b). The space group of the *Sc*Est crystal belonged to $P2_12_12_1$ with the following unit cell parameters: a = 50.23 Å, b = 68.69 Å, c = 71.15 Å and α, β, $\gamma = 90^\circ$. The initial structure of *Sc*Est was generated by molecular replacement using the CCP4i software suite [22]. Thermophilic carboxylesterase Est30 from *Geobacillus stearothermophilus* (PDB code, 1TQH) showed a high amino acid sequence similarity (61.79% identity) with ScEst, and was thus used as reference [23]. Model building and iterative structure refinement are currently underway using Coot software [24] and Refmac5 [25] in the CCP4i suite.

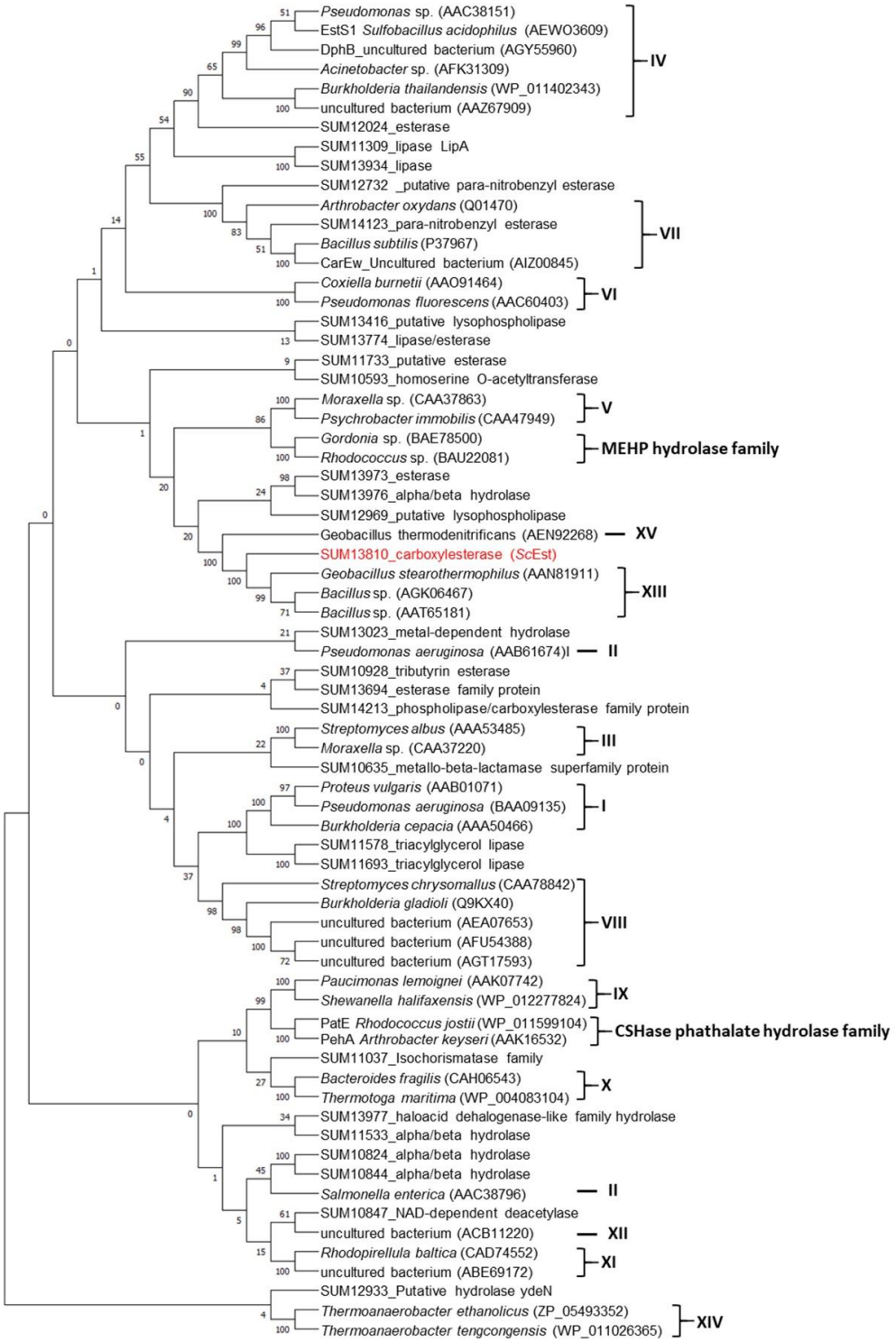

Figure 1. Phylogenetic analysis and classification of *Sc*Est with bacterial lipolytic enzyme families. Full-length protein sequences of 27 putative lipolytic enzymes from the *Staphylococcus chromogenes* strain NCTC10530 were aligned with bacterial lipolytic enzyme sequences of known categories using multiple sequence alignment (69 sequences). MEGA-X was used to create the phylogenetic tree using the neighbor-joining method. All unclear locations were deleted (using the pairwise deletion option). The percentage of duplicate trees in which the related taxa were clustered together in the bootstrap test (500 repetitions) appears next to each node. The GenBank accession numbers are indicated in parentheses.

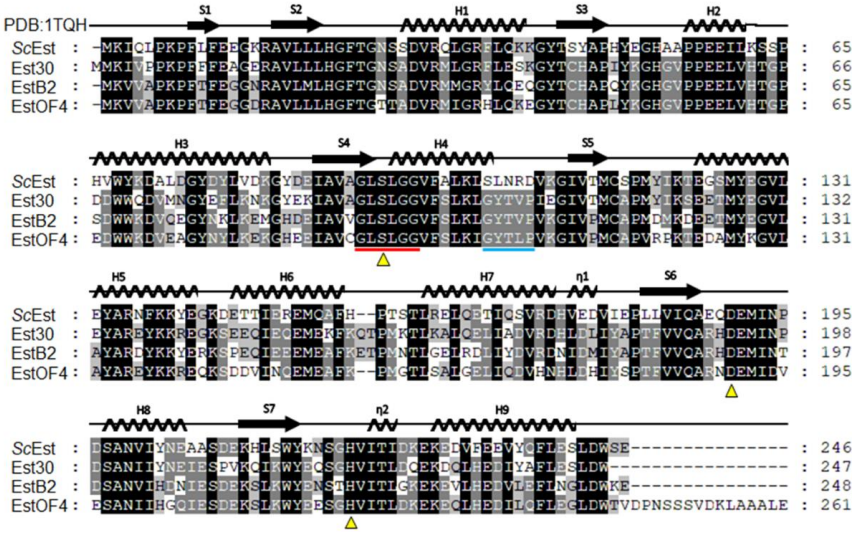

Figure 2. Multiple sequence alignment of *Sc*Est with other esterases of Family VIII. The sequences including that of thermostable carboxylesterase Est30 from *Geobacillus stearothermophilus* (GenBank AAN81911), EstOF4 from *Bacillus pseudofirmus* (GenBank AGK06467), and EstB2 from *Bacillus* sp. 01-855 (Genbank AAT65181) belonging to the bacterial lipolytic enzyme Family VIII were aligned using ClustalX. The conserved sites are highlighted in a darker color, whereas varied or polymorphic sites are shown in a lighter color. The secondary structure deduced from the Est30 structure (PDB code 1TQH) is displayed on the top of the aligned sequences. The conserved sequence at the active site characteristic of Family VIII is indicated with a red bar. The adjacent region specific to the *Sc*Est is marked with a cyan bar. The conserved catalytic triads are indicated with triangles.

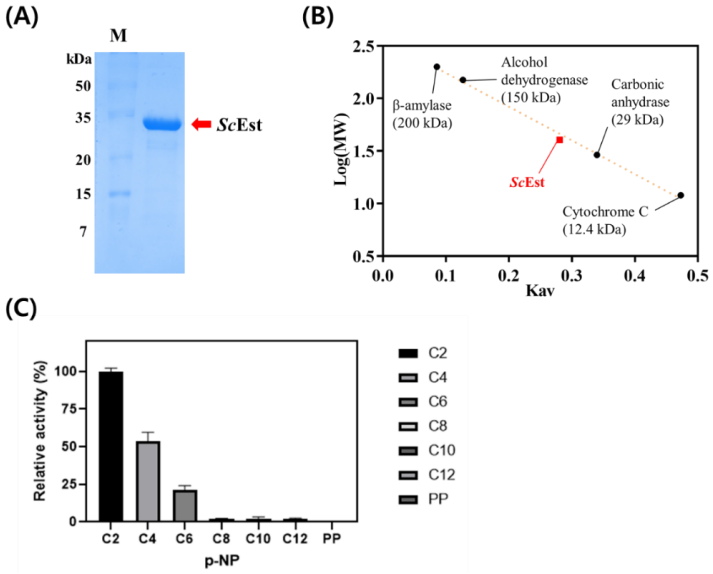

Figure 3. Purification and characterization of *Sc*Est. (**A**) SDS-PAGE of purified *Sc*Est along with a molecular weight marker. (**B**) Size-exclusion chromatography (SEC) of *Sc*Est. The elution time of *Sc*Est was integrated with the calibration curve obtained using molecular weight standards β-amylase (200 kDa), alcohol dehydrogenase (150 kDa), carbonic anhydrase (29 kDa), and cytochrome C (12 kDa). Kav = (Vs − Vo)/(Vc − Vo). vs. = elution time; Vo: column void volume; Vc: column volume. (**C**) Evaluation of esterase activity of *Sc*Est using 1 mM *p*-Nitrophenyl esters as substrates in 50 mM sodium phosphate buffer at pH 7.0. *p*-Nitrophenyl esters used in the activity assay were C2, *p*-Nitrophenyl acetate; C4, *p*-Nitrophenyl butyrate; C6, 4-Nitrophenyl hexanoate; C8, *p*-Nitrophenyl octanoate; C10, *p*-Nitrophenyl decanoate; C12, *p*-Nitrophenyl dodecanoate; PP, phenyl palmitate. The activity of recombinant *Sc*Est against *p*-NA(C2) is represented as 100%, whereas the relative activities against other substrates are shown in percentage.

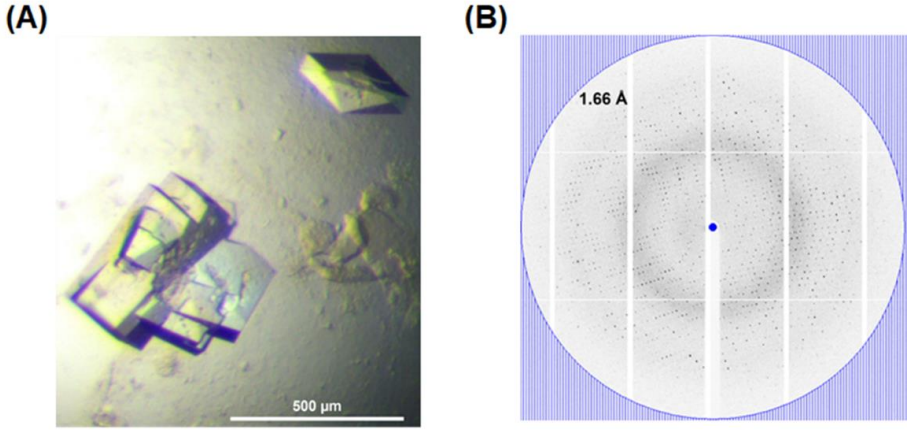

Figure 4. Preliminary X-ray crystallographic study of *Sc*Est. (**A**) *Sc*Est crystals for diffraction experiment obtained in 0.25 M ammonium citrate tribasic (pH 7.0), 20% PEG 3350. (**B**) Diffraction image of *Sc*Est crystal with the highest resolution value in the last atomic shell (1.69–1.66 Å). Blue circle represents the highest resolution range, and diffraction spots are shown at a resolution of 1.66 Å.

4. Conclusions

The biochemical characteristics of a carboxylesterase *Sc*Est, derived from *S. chromogenes* NCTC10530, which is the most common bacterial pathogen causing infectious diseases in dairy cows, were examined. The *ScEst* gene was identified, isolated, overexpressed in *E. coli*, and the protein was purified with affinity columns and size-exclusion chromatography. The *Sc*Est enzyme prefers the acyl derivatives with a short chain length as substrates. A preliminary crystallographic investigation of *Sc*Est resulted in a high-resolution dataset. We anticipate that elaborating the structure-based enzymatic mechanism of *Sc*Est will provide valuable information for understanding pathogenic esterases and designing ester prodrugs to treat MDR bacteria.

Author Contributions: Conceptualization, J.H.L. and T.D.K.; Methodology, J.H., W.Y. and S.J.; Validation, J.H., S.J., J.C. and K.K.K.; Formal Analysis, H.D. and M.J.L.; Writing—Original Draft Preparation, H.D., J.H. and T.D.K.; Writing—Review & Editing, H.D. and T.D.K.; Visualization, J.H. and S.J.; Supervision, H.D. and T.D.K.; Funding Acquisition, J.H.L. and T.D.K. All authors have read and agreed to the published version of the manuscript.

Funding: This research was a part of the project titled "Development of potential antibiotic compounds using polar organism resources (15250103, KOPRI Grant PM22030)" funded by the Ministry of Oceans and Fisheries, Republic of Korea. This research was also supported by a National Research Foundation of Korea Grant from the Korean Government (MSIT; the Ministry of Science and ICT) (NRF-2021M1A5A1075524) (KOPRI-PN22014), and an academic grant (NRF-2021R1F1A1048135) from the National Research Foundation of Korea (T.D.K).

Institutional Review Board Statement: Not applicable.

Informed Consent Statement: Not applicable.

Data Availability Statement: Not applicable.

Acknowledgments: We would like to thank the staff at the X-ray core facility of the Korea Basic Science Institute (KBSI; Ochang, Korea) and BL-7A of the Pohang Accelerator Laboratory (Pohang, Korea) for their kind help with data collection.

Conflicts of Interest: The authors declare no conflict of interest.

References

1. Nikaido, H. Multidrug resistance in bacteria. *Annu. Rev. Biochem.* **2009**, *78*, 119–146. [CrossRef] [PubMed]
2. Serra-Burriel, M.; Keys, M.; Campillo-Artero, C.; Agodi, A.; Barchitta, M.; Gikas, A.; Palos, C.; López-Casasnovas, G. Impact of multi-drug resistant bacteria on economic and clinical outcomes of healthcare-associated infections in adults: Systematic review and meta-analysis. *PLoS ONE* **2020**, *15*, e0227139. [CrossRef] [PubMed]

3. Zárate, S.G.; De La Cruz Claure, M.L.; Benito-Arenas, R.; Revuelta, J.; Santana, A.G.; Bastida, A. Overcoming aminoglycoside enzymatic resistance: Design of novel antibiotics and inhibitors. *Molecules* **2018**, *23*, 284. [CrossRef] [PubMed]
4. Fair, R.J.; Tor, Y. Antibiotics and bacterial resistance in the 21st century. *Perspect. Medicin. Chem.* **2014**, *6*, 25–64. [CrossRef] [PubMed]
5. Jubeh, R.; Breijyeh, B.; Karaman, Z. Antibacterial prodrugs to overcome bacterial resistance. *Molecules* **2020**, *25*, 1543. [CrossRef]
6. Sakagami, K.; Atsumi, K.; Tamura, A.; Yoshida, T.; Nishihata, K.; Fukatsu, S.J. *Antibiot.* Synthesis and oral activity of ME 1207, a new orally active cephalosporin. *J. Antibiot.* **1990**, *8*, 8–11. [CrossRef]
7. Maag, H. *Prodrugs of Carboxylic Acids, Prodrugs*; Springer: New York, NY, USA, 2008; pp. 703–729. [CrossRef]
8. Hamada, Y. Recent progress in prodrug design strategies based on generally applicable modifications. *Bioorg. Med. Chem. Lett.* **2017**, *27*, 1627–1632. [CrossRef]
9. Elayyan, S.; Karaman, D.; Mecca, G.; Scrano, L.; Bufo, S.A.; Karaman, R. Antibacterial predrugs-from 1899 till 2015. *World J. Pharm. Pharm. Sci.* **2015**, *4*, 1504–1529. [CrossRef]
10. Larsen, E.M.; Johnson, R.J. Microbial esterases and ester prodrugs: An unlikely marriage for combating antibiotic resistance. *Drug Dev. Res.* **2019**, *80*, 33–47. [CrossRef]
11. Satoh, T.; Hosokawa, M. Structure, function and regulation of carboxylesterases. *Chem. Biol. Interact.* **2006**, *162*, 195–211. [CrossRef]
12. Mikati, M.O.; Miller, J.J.; Osbourn, D.M.; Barekatain, Y.; Ghebremichael, N.; Shah, I.T.; Burnham, C.D.; Heidel, K.M.; Yan, V.C.; Muller, F.L.; et al. Antimicrobial prodrug activation by the Staphylococcal glyoxalase GloB. *ACS Infect. Dis.* **2020**, *6*, 3064–3075. [CrossRef] [PubMed]
13. Wang, Y.; Le, L.T.H.L.; Yoo, W.; Lee, C.W.; Kim, K.K.; Lee, J.H.; Kim, T.D. Characterization, immobilization, and mutagenesis of a novel cold-active acetylesterase (EaAcE) from Exiguobacterium antarcticum B7. *Int. J. Biol. Macromol.* **2019**, *136*, 1042–1051. [CrossRef] [PubMed]
14. Oh, C.; Ryu, B.H.; An, D.R.; Nguyen, D.D.; Yoo, W.; Kim, T.; Ngo, T.D.; Kim, H.S.; Kim, K.K.; Kim, T.D. Structural and biochemical characterization of an octameric carbohydrate acetylesterase from *Sinorhizobium meliloti*. *FEBS Lett.* **2016**, *590*, 1242–1252. [CrossRef] [PubMed]
15. Lee, C.W.; Kwon, S.; Park, S.H.; Kim, B.Y.; Yoo, W.; Ryu, B.H.; Kim, H.W.; Shin, S.C.; Kim, S.; Park, H.; et al. Crystal structure and functional characterization of an esterase (EaEST) from exiguobacterium antarcticum. *PLoS ONE* **2017**, *12*, e0169540. [CrossRef] [PubMed]
16. Sarkar, J.; Dutta, A.; Pal Chowdhury, P.; Chakraborty, J.; Dutta, T.K. Characterization of a novel family VIII esterase EstM2 from soil metagenome capable of hydrolyzing estrogenic phthalates. *Microb. Cell Fact.* **2020**, *19*, 77. [CrossRef] [PubMed]
17. Arpigny, J.L.; Jaeger, K.E. Bacterial lipolytic enzymes: Classification and properties. *Biochem. J.* **1999**, *343*, 177–183. [CrossRef]
18. Hitch, T.C.A.; Clavel, T. A proposed update for the classification and description of bacterial lipolytic enzymes. *PeerJ* **2019**, *7*, e7249. [CrossRef]
19. Larkin, M.A.; Blackshields, G.; Brown, N.P.; Chenna, R.; Mcgettigan, P.A.; McWilliam, H.; Valentin, F.; Wallace, I.M.; Wilm, A.; Lopez, R.; et al. Clustal W and Clustal X version 2.0. *Bioinformatics* **2007**, *23*, 2947–2948. [CrossRef]
20. Kumar, S.; Stecher, G.; Li, M.; Knyaz, C.; Tamura, K. MEGA X: Molecular evolutionary genetics analysis across computing platforms. *Mol. Biol. Evol.* **2018**, *35*, 1547–1549. [CrossRef] [PubMed]
21. Peng, Y.; Fu, S.; Liu, H.; Lucia, L.A. Accurately determining esterase activity via the isosbestic point of p-nitrophenol. *BioResources* **2016**, *11*, 10099–10111. [CrossRef]
22. Vagin, A.; Teplyakov, A. Molecular replacement with MOLREP. *Acta Crystallogr. D Biol. Crystallogr.* **2010**, *66*, 22–25. [CrossRef]
23. Liu, P.; Wang, Y.F.; Ewis, H.E.; Abdelal, A.T.; Lu, C.D.; Harrison, R.W.; Weber, I.T. Covalent reaction intermediate revealed in crystal structure of the Geobacillus stearothermophilus carboxylesterase Est30. *J. Mol. Biol.* **2004**, *342*, 551–561. [CrossRef]
24. Winn, M.D.; Ballard, C.C.; Cowtan, K.D.; Dodson, E.J.; Emsley, P.; Evans, P.R.; Keegan, R.M.; Krissinel, E.B.; Leslie, A.G.W.; McCoy, A.; et al. Overview of the CCP4 suite and current developments. *Acta Crystallogr. D Biol. Crystallogr.* **2011**, *67*, 235–242. [CrossRef]
25. Murshudov, G.N.; Skubák, P.; Lebedev, A.A.; Pannu, N.S.; Steiner, R.A.; Nicholls, R.A.; Winn, M.D.; Long, F.; Vagin, A.A. REFMAC5 for the refinement of macromolecular crystal structures. *Acta Crystallogr. D Biol. Crystallogr.* **2011**, *67*, 355–367. [CrossRef]